

# CT and MR imaging of odontoid abnormalities: A pictorial review

Nishchint Jain, Ritu Verma, Umesh C Garga, Barinder P Baruah, Sachin K Jain<sup>1</sup>, Surya N Bhaskar<sup>2</sup>

Departments of Radio-Diagnosis, <sup>1</sup>Medicine and <sup>2</sup>Neurosurgery, Postgraduate Institute of Medical Education and Research (PGIMER and RML), Dr. Ram Manohar Lohia Hospital, New Delhi, India

**Correspondence:** Dr. Nishchint Jain, Department of Neuro-Radiology, All India Institutes of Medical Sciences, New Delhi, India.  
E-mail: nishchintjain@gmail.com

## Abstract

Odontoid process is the central pillar of the craniovertebral junction. Imaging of this small structure continues to be a challenge for the radiologists due to complex bony and ligamentous anatomy. A wide range of developmental and acquired abnormalities of odontoid have been identified. Their accurate radiologic evaluation is important as different lesions have markedly different clinical course, patient management, and prognosis. This article seeks to provide knowledge for interpreting appearances of odontoid on computed tomography (CT) and magnetic resonance imaging (MRI) with respect to various disease processes, along with providing a quick review of the embryology and relevant anatomy.

**Key words:** Anterior longitudinal ligament; atlanto-axial dislocation; atlanto-dental interval; basilar invagination; computed tomography; cranio-vertebral junction; fracture; magnetic resonance imaging; odontoid; posterior longitudinal ligament; transverse atlantal ligament

## Introduction

The odontoid process is a part of the C2 or axis vertebra and forms pivot of the structures forming the craniovertebral junction (CVJ). The pathologies of odontoid can be congenital or acquired. Congenital anomalies include various types of odontoid dysgenesis such as os odontoideum, condylus tertius, persistent os-terminale, and odontoid aplasia. Acquired anomalies of odontoid may be traumatic, degenerative, inflammatory or neoplastic in nature [Table 1].<sup>[1,2]</sup> Atlanto-axial dislocation (AAD) and basilar invagination (BI) may be seen in both congenital and acquired conditions. Symptoms may refer to the cervical spinal cord, brainstem, cerebellum, cervical nerve roots, lower cranial nerves, and the vascular supply to these structures or the adjacent cerebrospinal fluid (CSF) channels.<sup>[3]</sup>

## Techniques of Evaluation

The complex anatomy of this region requires careful evaluation of bony as well as ligamentous structures in all three planes; therefore, cross-sectional studies are the mainstay. However, conventional radiography still plays an important role in initial evaluation. Recommended radiographic views are open mouth, anteroposterior (AP), lateral, and flexion-extension views. Anatomical landmarks, parameters, and relationships [Table 2] that were originally described on conventional radiographs<sup>[4-6]</sup> and form the basis of craniometry [Figure 1] have been extrapolated for use with computed tomography (CT) and magnetic resonance imaging (MRI).

Multidetector computed tomography (MDCT) with isotropic resolution and multiplanar reformations has

This is an open access article distributed under the terms of the Creative Commons Attribution-NonCommercial-ShareAlike 3.0 License, which allows others to remix, tweak, and build upon the work non-commercially, as long as the author is credited and the new creations are licensed under the identical terms.

**For reprints contact:** reprints@medknow.com

**Cite this article as:** Jain N, Verma R, Garga UC, Baruah BP, Jain SK, Bhaskar SN. CT and MR imaging of odontoid abnormalities: A pictorial review. Indian J Radiol Imaging 2016;26:108-19.

### Access this article online

#### Quick Response Code:



**Website:**  
www.ijri.org

**DOI:**  
10.4103/0971-3026.178358

**Table 1: Pathological conditions affecting odontoid**

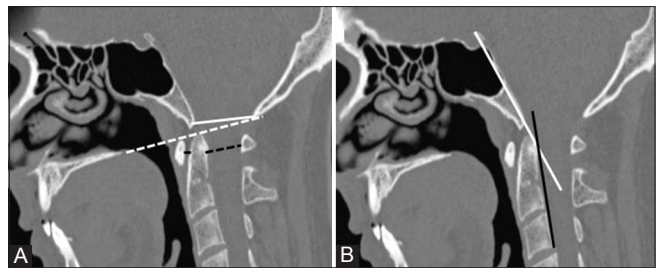
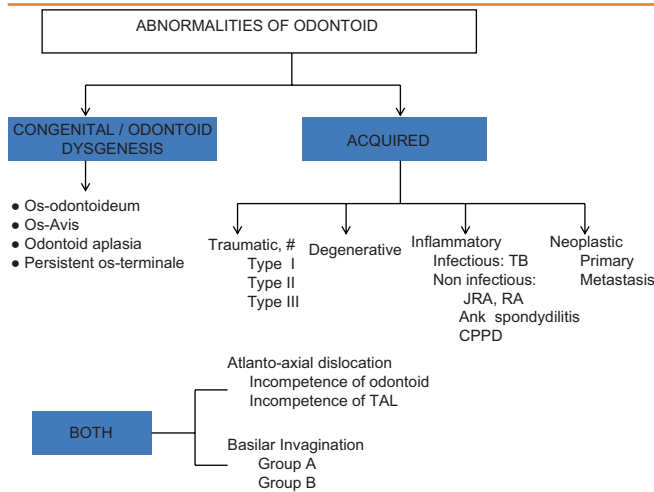


**Figure 1 (A and B):** Craniometric measurements (A) Solid black: ADI normal is <3 mm adults and <5 mm children, Dotted black: PADI normal is >13 mm Dotted white: Chamberlain's line and solid white: Mc Rae Line (B) White: Wecken-Heim Clivus base line: It should fall tangent to the posterior aspect of the tip of the odontoid. It forms Clivus Canal angle along the posterior surface of the axis body

**Table 2: Basic craniometry**

Craniometric measurement	Anatomic landmarks	Normal values and clinical implications
ADI	From posterior border of anterior arch to anterior surface of dens	>3mm in adults and >5mm in children indicates AAD
PADI	From posterior surface of dens to anterior border of posterior tubercle	<13 mm indicates canal narrowing
Chamberlains line	Line joining basion to opisthion	Dens projecting > 6 mm above it indicates Basilar Invagination
Mc Rae line	Line joining anterior and posterior margins of foramen magnum	Odontoid tip lying above this line is indicative of type A Basilar Invagination
Wecken-Heim Clivus base line	Line drawn along clivus and extending into upper cervical canal, It should be tangent to odontoid	If it intersects the body of dens anterior craniocervical dislocation is present and vice versa
Clivus canal angle	The angle formed by the Wackenheim line and a line constructed along the posterior surface of the axisbody and odontoid process	Normal is 150-180. If <150 ventral cord compression may occur

ADI: Atlanto-dental interval, PADI: Posterior atlantodental interval

enabled better visualization of complex bony abnormalities. It also helps with craniometric measurements that cannot be accounted by plain radiographs.

At our institution, CT was done on a 40-slice MDCT scanner. Imaging parameters were as follows: 0.5 mm slice thickness, 0.75 s/rotation, 120 kV, and 300 mA. Reconstruction was done with a slice thickness of 1.0 mm.

Due to its multiplanar capabilities and excellent delineation of neural structures and ligaments, MRI has become the imaging modality of choice.<sup>[7]</sup> Dynamic MRI<sup>[8]</sup> in flexion, extension, and neutral positions offers special role in diagnosis of AAD. 2D and 3D time-of-flight (TOF) methods

can help in detection of underlying vascular pathology. Phase-contrast CSF flow study aids further in surgical decision-making and patient management.<sup>[9,10]</sup>

All patients were examined at our institution by using 1.5 T MR scanner in neutral positioning and spine coil. The imaging parameters were: T1 and T2 turbo spin-echo with a repetition time (TR)/echo time (TE) of 400/15 and 2000/110 ms, respectively; section thickness/gap was 3.0/0.3 mm; field of view (FOV) 260 × 220 mm; and matrix size 288 × 256. Standard sagittal T1, T2; axial T1, T2 and gradient echo (GRE) and coronal T2W sequences were taken. TOF, flexion-extension, and PC-CSF flow study was done wherever indicated.

### Relevant Anatomy

The odontoid process projects cephalad from its articulation with the axis body. On the ventral surface is an oval facet, which articulates with the dorsal surface of anterior arch of atlas. In the dorsal aspect of the dens is a transverse groove over which passes the transverse ligament of the atlas (TAL) [Figure 2].

### Primary Stabilizing Ligaments

TAL, is essentially horizontal limb of cruciate ligament. It represents a fibrocartilagenous surface ventrally, allowing a free gliding motion to occur over the posterior facet of the dens.<sup>[11,12]</sup> TAL effectively limits anterior translation and flexion of the atlanto-axial (AA) joint.

Alar ligaments are two strong cords that attach to the dorsolateral body of the dens. These fibers extend laterally and rostrally. They are ventral and cranial to the transverse ligament. Alar ligament allows an anterior shift of C1 from 3 to 5 mm.

### Secondary Stabilizing Ligaments

#### Tectorial membrane

It is the rostral extension of the posterior longitudinal ligament of the vertebral column and is essential for limiting

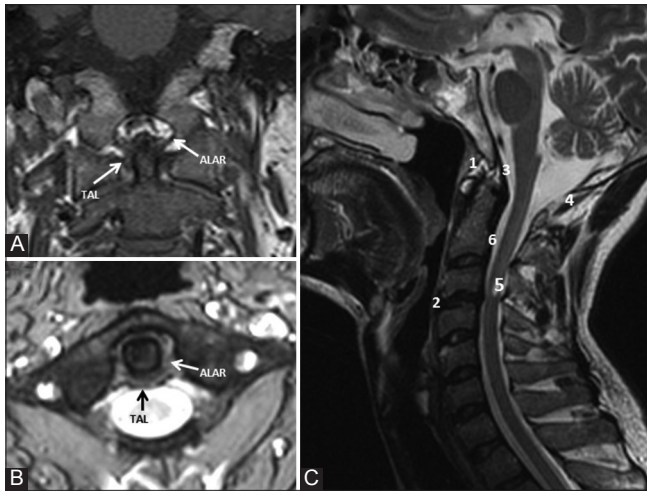


**Figure 2 (A-C):** Coronal (A) and axial (B) T2W image showing major primary stabilising and sagittal T2W image (C) showing the various secondary stabilising ligaments in relation to odontoid and CVJ. TAL = Transverse atlantal ligament, 1: Anterior atlanto-occipital membrane, 2: ALL, 3: Tectorial membrane, 4: Posterior atlanto-occipital membrane, 5: Ligamentum flavum, 6: PLL

flexion. The accessory bands of the ligament passing to the lateral capsule of the AA joints form the Arnold's ligament.

*Apical ligament* is a small, slender band of fibers containing small amount of collagen and elastin. It has no mechanical significance.

Other less important secondary stabilizers are anterior and posterior atlanto-occipital membranes and anterior and posterior longitudinal ligaments.

### Atlantoaxial dislocation

Increased atlanto-dental interval (ADI; >3 mm in adults and >5 mm in children) is diagnostic of AAD. According to Greenberg's classification, AAD may be due to incompetence of odontoid (congenital, traumatic, infectious, or tumorous) or incompetence of TAL (congenital, traumatic, or inflammatory) [Figure 3].

### Basilar invagination

Dens projecting 6 mm above Chamberlain's line is diagnostic of BI. It is not a pathology of odontoid itself; however, it can lead to disturbed craniometric relationship of dens and cervicomedullary compression. BI can be seen in a variety of conditions [Figure 4]. It is of two types: Group A when there is violation of Chamberlain's line along with disturbance of McRae line and group B when there is violation of Chamberlain's line without disturbance of McRae line.

### Embryology and Developmental Anomalies of Odontoid

The development of odontoid is complex. The top of the dens develops from the proatlans which is cranial half of the

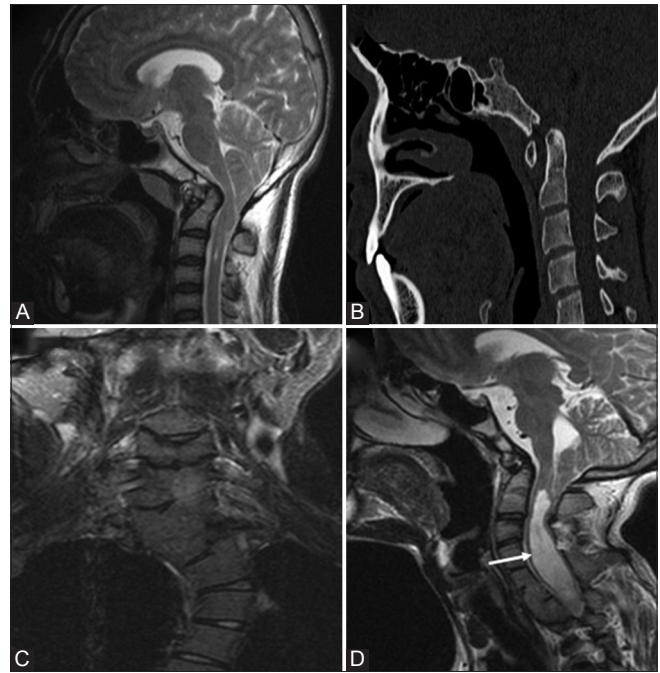


**Figure 3 (A-D):** AAD in two different patients Chiari 1 malformation: Sagittal T1W (A) and CT (B) image showing descent of cerebellar tonsil beyond foramen magnum into the cervical canal. Associated basilar invagination, atlanto-axial dislocation and occipitalisation of atlas is seen Klippel feil syndrome: Coronal (C) Sagittal T2W (D) MRI images in a patient with short neck showing multiple segmentation anomalies with AA dislocation occipitalisation of atlas, and chiari I malformation. Associated syrinx (arrow) is also noted

first cervical sclerotome.<sup>[13,14]</sup> The rest of the dens develops from the caudal half of the first cervical sclerotome. Body and neural arches of the axis develop from the second cervical sclerotome.<sup>[15,16]</sup> Proatlans also forms the anterior margin of foramen magnum, occipital condyles and third condyle of the occipital bone similarly caudal portion of the first cervical sclerotome also forms lateral masses and posterior arch of atlas. Therefore, odontoid dysgenesis is frequently associated with anomalies of basiocciput and atlas. The cruciate and alar ligaments are condensation of the lateral portion of proatlans [Table 3].

Four ossification centers are present at birth for axis vertebra: One for each neural arch, one for the body, and one for the odontoid. *In utero*, the dens has two ossification centers in the midline, which fuse by the 7<sup>th</sup> month of intrauterine life.<sup>[17]</sup> A secondary ossification center appears at the apex (the terminal ossicle) at 3-6 years of age and fuses with the rest of the dens by 12 years of age.<sup>[17]</sup> Posteriorly, the neural arches fuse by 2-3 years of age. In a young child, the unossified portions of the odontoid may give the false impression of odontoid hypoplasia.<sup>[18]</sup> Similarly, one may erroneously conclude that the child has C1-2 instability, because the anterior arch of the atlas commonly may slide upward and protrude beyond the ossified portion of the odontoid on the lateral extension radiograph.

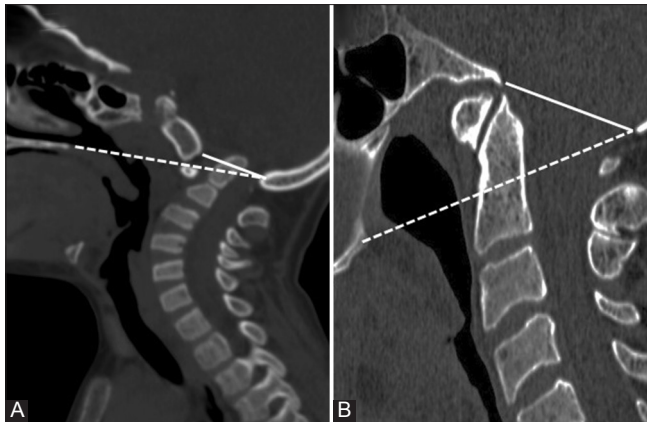
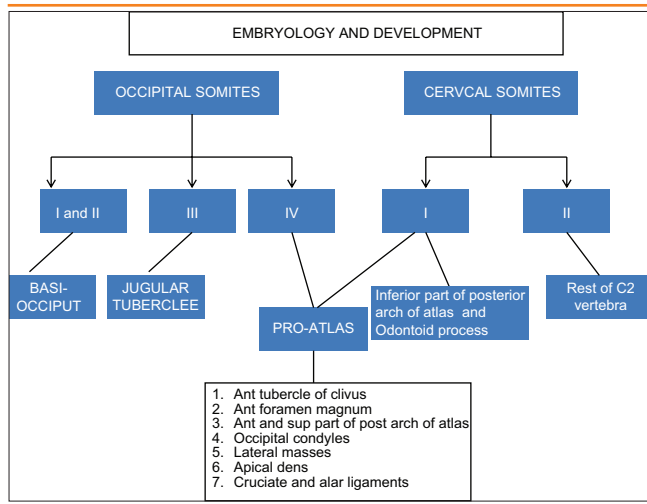


**Figure 4 (A and B):** Sagittal CT images (A) and (B) showing Group A and Group B Basilar Invagination respectively. *Dotted-* Chamberlain's line; *Solid-* Mc Rae Line

**Table 3: Embryology of odontoid**



**Neural central synchondrosis**

At birth, the odontoid process is separated from the body of the axis vertebra by a cartilaginous band that represents the epiphyseal growth plate or lateral synchondrosis.<sup>[19,20]</sup> The synchondrosis lies below the level of the superior articular facets of the axis and does not represent anatomical base of the dens [Figure 5]. This synchondrosis is present in most children younger than 3-4 years of age and disappears by 8 years of age.<sup>[21]</sup> It rarely persists into adolescence and adult life and if present, the line is not seen at the base of the dens where a fracture would be anticipated, but lies well below the level of the superior articular facets within the body of the axis.<sup>[17]</sup>

**Odontoid aplasia/hypoplasia**

Complete agenesis of odontoid is extremely rare<sup>[17,22]</sup> and usually occurs in the context of collagenopathy syndromes such as spondyloepiphyseal and spondylometaphyseal dysplasias.<sup>[17]</sup> It appears as slight depression<sup>[23]</sup> between the superior articular facets on open mouth view [Figure 6].

Agenesis or hypogenesis of just the basal segment results in a stumpy dental pivot with a floating apical ossicle. Both types are associated with AA instability. Dynamic CT scans in flexion and extension should be done as many patients have been found with significant posterior subluxation. AA instability and resultant stroke due to vascular compression<sup>[24]</sup> may also occur. Agenesis of only the apical segment is far more common by comparison.<sup>[17]</sup> Radiographically, the dens is short, although there is usually adequate pivot height for the transverse atlantal ligament, and thus, there is no instability.<sup>[17]</sup> Treatment of symptomatic cases is usually C1-C2 fusion.

**Os odontoideum**

It is the most common developmental anomaly of odontoid. The definition of an os odontoideum is uniform throughout the literature: An ossicle with smooth circumferential cortical margins representing the odontoid process that has no osseous continuity with the body of C2.<sup>[25]</sup> The origin of os odontoideum remains debated in the literature with evidence for both acquired and congenital causes.<sup>[25]</sup> Two types have been described in the literature: Orthotopic and dystopic. In os odontoideum, there is a joint-like articulation between the odontoid and the body of the axis that appears radiologically as a wide radiolucent gap that may be confused with the normal neurocentral synchondrosis before 5 years of age. Therefore, in children, the diagnosis of os odontoideum is confirmed by showing relative motion between the odontoid and the body of the axis. In adults, the diagnosis of os odontoideum is suggested by observing a smooth radiolucent defect between the dens and the body of the axis. Associated cruciate ligament incompetence and AA instability are commonly seen. When present, instability may lead to substantial narrowing of the spinal canal and cord compression at the level of C1.

Occasionally, differentiation between an os odontoideum and a type 2 odontoid fracture on a lateral radiograph may be problematic. In os odontoideum, the gap between the free ossicle and the axis usually extends above the level of the superior facets and is wide with a smooth edge. The ossicle is round to oval with uniform cortical thickness and is approximately half the size of odontoid [Figure 7]. The odontoid ossicle is fixed firmly to the anterior ring of the atlas and moves with it in flexion, extension, and lateral slide. The anterior portion of the atlas is usually hypertrophied and rounded, rather than half-moon shaped,<sup>[16,26]</sup> while the posterior portion of the ring may be hypoplastic or absent. The axis body has a well corticated with convex upper margin. In traumatic nonunion, the gap between the fragments is characteristically narrow and irregular and frequently extends into the body of the axis below the level of the superior facets of the axis [Figure 8]. The bone fragments appear to “match” with the odontoid defect and there is no marginal cortex at the level of the fracture or the rounded-off appearance found with os odontoideum.

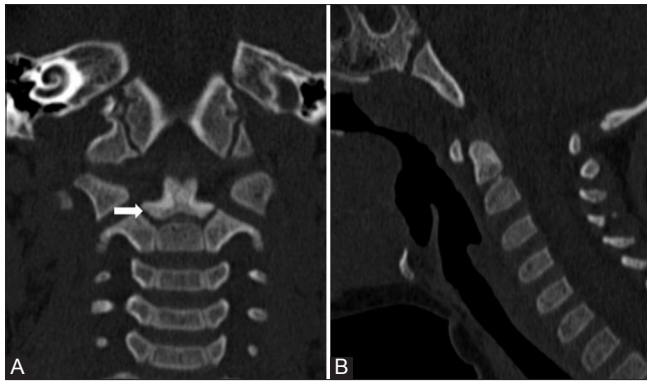


**Figure 5 (A and B): Neural Central Synchondrosis:** Coronal (A) and Sagittal (B) reformatted CT images showing ossification of dens in 4 year old child. The tip of basal dental segment is bicornuate from bilateral secondary ossification centres. Lucent gap (arrow) marks synchondrosis which fuses normally fuses with rest of the C2 by 8 years of age. Note terminal ossicle has not appeared yet

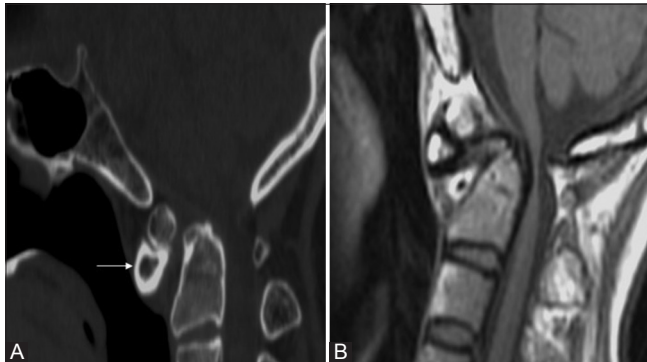


**Figure 7 (A and B): Os odontoideum:** Sagittal CT image (A) T1W MRI (B) in a 17 year old patient with quadriplegia showing rounded bony fragment lying above and anterior to the base of dens. Dens is hypoplastic, smooth and well corticated and anterior arch is hypertrophied (arrow) and rounded differentiating the condition from fracture. MR also revealed marked ligament thickening, spinal canal narrowing with cord compression and myelomalacic changes

Condylus tertius [Figure 8] is another important differential for os odontoideum. It occurs due to failure of fusion of proatlans with occipital sclerotomes that forms clivus, as a result the clivus is small and blunted.<sup>[17]</sup> A separate bony tubercle is seen which is firmly attached to basion and frequently forms true synovial joint with anterior arch of C1 and odontoid apex. This bony tubercle may sometimes cause neural compression. As it makes the accessory or third joint between atlas and occiput it is aptly termed as median or third occipital condyle (condylus tertius).

Common indications for surgical stabilization include os odontoideum in association with occipitocervical pain, myelopathy, severe C1-2 instability, and other associated osseous anomalies. Neural decompression must address the anterior bony or soft tissue impingement of the spinal cord or compression posteriorly from the dorsal arch of C1.

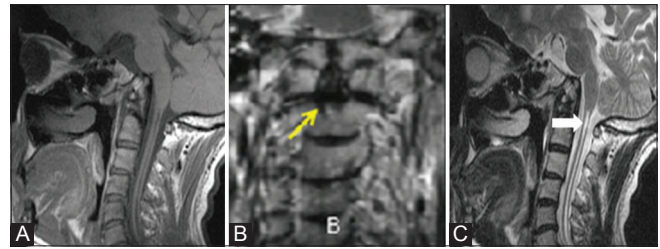


**Figure 6 (A-C): Odontoid aplasia:** Sagittal T1W (A) and coronal (B) and sagittal T2W (C) MR images of 28 year old patient with aplastic dens. Excavation defect is seen in the body of odontoid (arrow) below the level of articular process on coronal image. Additional findings include platybasia, short clivus and syrinx (solid arrow) involving the cervical spinal cord

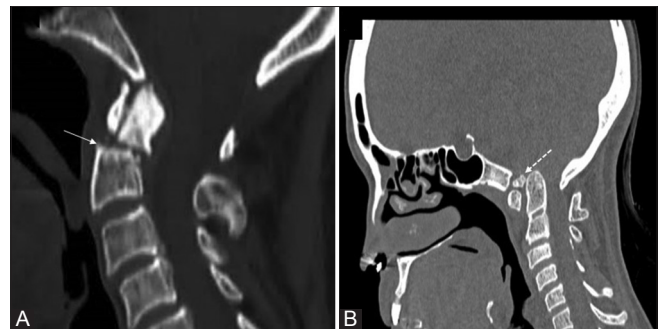


**Figure 8 (A and B): Type II fracture (A)** Sagittal CT in a 56 year old patient with trauma showing the fracture fragment that match with the expected defect, the upper margins of axis are sharp and irregular (solid arrow) with normal half moon shaped anterior arch. **Condylus Tertius (B)** Sagittal CT image in a 39 year old female patient showing an accessory ossification centre (dotted arrow) is seen forming a pseudo-articulation with anterior arch of atlas. The distal most end of clivus is blunted while dens is normal. Note occipitalisation of posterior arch atlas and BI

*Persistent os-terminale* results from failure of fusion of the terminal ossicle to the remainder of the odontoid process.<sup>[16]</sup> This anomaly is stable when isolated because the TAL's anchorage is not affected and is of relatively little clinical significance. The odontoid process is usually normal in height. On occasion, it may be confused with a type 1 odontoid fracture (avulsion of the terminal ossicle), and absolute differentiation between the two entities may be difficult [Figure 9].

Although most ossiculum terminales are stable anomalies, cases have been described in which the basal dental segment is hypoplastic and the dental pivot is short leading to AA subluxation and high cord compression. Posterior C1-C2 fusion is adequate treatment if complete reduction is achievable. If there is persistent anterior dislocation of C1, its posterior arch may have to be removed for decompression, in which case occipital C2-C3 fusion is necessary.<sup>[17]</sup>

#### Dens bicornis

The tip of the basal dental segment is bicornuate from bilateral secondary ossification centers. Small density above



**Figure 9:** *Persistent os-terminale*: The terminal ossicle is seen separate from dens due to failure of fusion. It may be confused with a type 1 odontoid fracture. The odontoid process is usually normal in height

this represents early third wave of ossification within the apical dental segment which is not ossified at birth and hence not observed,<sup>[17]</sup> but it usually appears at 3 years of age. Ossification of the dental tip and bony fusion of the upper synchondrosis are not completed until adolescence. Dens bicornis results from aberrant distal ossification leading to failure of development of apical dental segment, i.e., the terminal ossicle [Figure 10].

A completely bifid dens is an extremely rare entity. It is different from the “dens bicornis” described by von Torklus and Gehle in which only the tip of the dens is bicornuate and the function of the otherwise well-formed dental pivot is unaffected.<sup>[27]</sup> In true dental bifidity, the partition in the basal dental segment goes full length of the process to the lower synchondrosis.

#### Os avis

The apical dental segment is attached to basiocciput and not fused to main dental stem due to abnormal resegmentation of proatlant centrum.<sup>[28]</sup> Pivot is shortened, but firmly fixed to axis centrum where a semi-lucent line representing the lower synchondrosis marks the successful integration of the two lower dens-axis components. In literature this anomaly has been overlapped with dystopic os-odontoidum.<sup>[17,27]</sup>

#### Anteverted odontoid

Anteversion of odontoid is the angulation anomaly seen at the synchondrosis of C2 body and odontoid process.

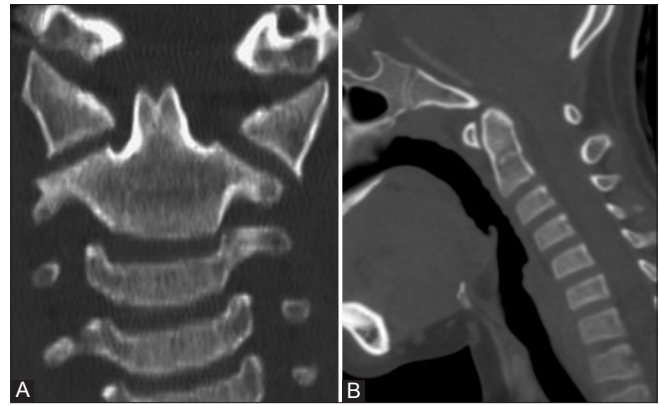


**Figure 10 (A and B):** *Dens bicornis*: Reformatted coronal and Sagittal CT (A and B) images in a 19 year old asymptomatic boy showing bifid tip of the dens. Note that lower synchondrosis has also closed and terminal ossicle has not appeared yet. Note that dens pivot is of normal height

Anteversion angle is the angle formed by connecting a line through the base of the axis to the line drawn through the tip of the odontoid process normal angle varies between 60 to 105 degrees (mean 95). There is an increased chance of cord compression by the body of axis (the offending element) rather than the tip of the odontoid.<sup>[28]</sup> According to the proposed hypothesis, this anomaly results from traction by the apical ligament over the tip of the odontoid process during the early developmental stages of CVJ when the apical ligament is thick and active. Management guidelines are decompression of the offending body portion followed by occipitocervical fusion.

## Acquired Abnormalities

### Fractures

Fracture odontoid constitutes about 7-14% of cervical spine fractures.<sup>[29]</sup> Flexion is the most common mechanism of injury causing anterior displacement of C1 on C2. Odontoid fractures are classified into three types according to Anderson and D'Alonzo classification [Figure 11].

Type I (<5%): Oblique avulsion fracture through the upper part of the odontoid process at the point of alar ligament attachment. It is usually stable, but may be associated with AAD.

Type II (>60%): Fracture occurring at the junction of the odontoid process and the body of axis [Figure 12].

Type III (30%): Fracture line extends down into the body of axis.<sup>[30]</sup> It does not actually involve dens. The fracture is unstable as atlas and occiput move together as a unit.

Fielding *et al.*<sup>[31]</sup> suggested that a greater than 3 mm separation between the anterior C-1 ring and the dens implies possible transverse ligament disruption. According

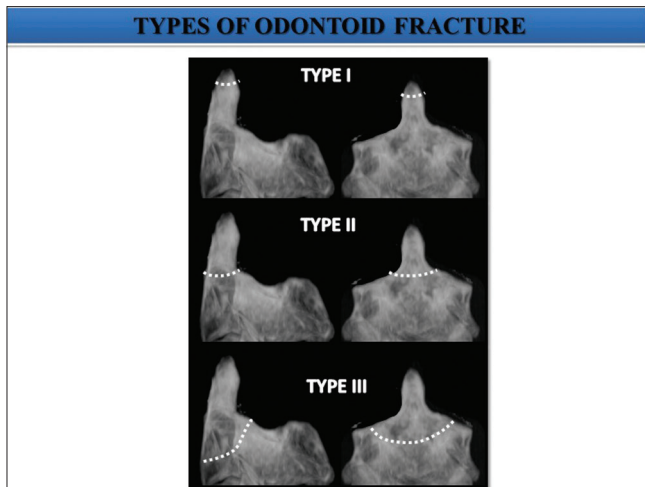


**Figure 11:** Anderson and D'Alonzo classification of three types of odontoid fractures (#) Type I: Oblique avulsion # through the upper part of the odontoid process at the point of alar ligament attachment. Type II: # occur at the junction of the odontoid process and the body of axis. Type III: # line extend down in to the body of axis

to Spence *et al.*,<sup>[32]</sup> when the lateral masses of the atlas overhang the superior articular facets of the axis by more than 7 mm, injury of this ligament may similarly occur. A type III odontoid fracture can be differentiated from type II fracture by disruption of odontoid ring on AP and lateral radiographs in the latter<sup>[33]</sup> [Figure 13].

The use of CT with both sagittal and coronal CT reconstructions is quite helpful in demonstrating the plane of the fracture line as well as the degree of comminution. MRI has a more limited role in evaluating patients who have sustained odontoid fractures. However, evaluation of the integrity of the transverse ligament can be facilitated using MRI, but is not usually recommended in neurologically stable patients.<sup>[34]</sup>

#### Rotatory AA subluxation/fixation

Rotatory AAD most commonly occurs after trauma and patients classically present with torticollis. The other less common cause is post-respiratory tract infection. Fielding and Hawkins classify AA rotatory subluxation into four types: Type I- Rotatory fixation without anterior displacement of the atlas. Type II- Rotatory fixation with anterior displacement of the atlas of 3-5 mm. Type III- Rotatory fixation with anterior displacement of more than 5 mm. Type IV- Rotatory fixation with posterior displacement.

In a normal patient, the septal axis<sup>[35]</sup> along the nasal septum should be perpendicular to the transverse axis of C1, AP axis of C1 should remain parallel to the AP axis of head through foramen magnum, and AP axis of C1 and C2 should be parallel. While in rotatory AA fixation, these relationships are not maintained [Figure 14].

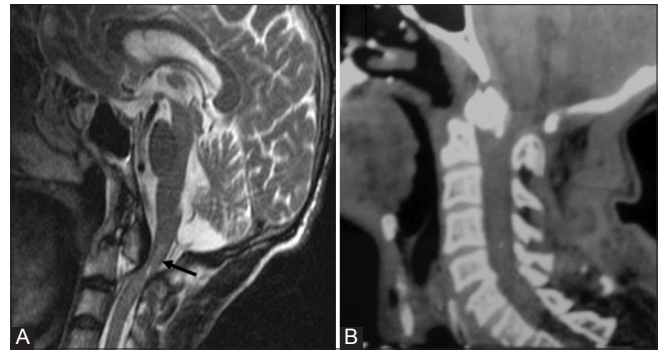


**Figure 12 (A and B):** Type II fracture Odontoid: Sagittal T2W (A) and reformatted sagittal CT (B) of 58 year old male showing type 2 odontoid fracture with retropulsion of proximal segment posteriorly. There is injury to posterior longitudinal ligament, cord compression with marrow edema

On AP radiographs, C1 appears rotated over C2 and the distance between the odontoid and lateral masses of C1 becomes asymmetric. CT with head rotated as far to the left and right as possible during scanning can demonstrate fixed position of atlas with respect to axis and loss of normal rotation at the AA joint. According to Kawalski *et al.*,<sup>[35]</sup> demonstration of cervical rotation without movement at C1-C2 is necessary to establish the diagnosis of rotatory fixation.

#### Degenerative spondylitis

Approximately 50% of the axial rotation of the cervical spine occurs at C1-C2 articulation, hence facet joints are involved in almost every head movement. Most commonly, pain is localized to the upper posterior neck, which is exacerbated with axial rotation, but not flexion-extension. Open mouth odontoid view is diagnostic in most cases, whereas flexion-extension radiographs, CT scan, bone scan, and MRI can be useful in AA joint instability. Characteristic features of degenerative joint disease are evident, showing reduced ADI with sclerosis and osteophyte formation<sup>[36,37]</sup> which are better appreciated on T1W images. Fluid signal may be noted in predental space, which normally contains fat/soft tissue [Figure 15]. A reduction in the height of the AA lateral mass complex, mobile AAD, and BI are the most frequently encountered radiological features with instability.<sup>[38]</sup>

#### Tuberculosis

Spinal tuberculosis (TB) accounts for only 1% of all TB cases, 6% of extrapulmonary TB, and 50% of skeletal TB.<sup>[38]</sup> The plain film changes are generally seen after about 50% of the bone is destroyed and may take as much as 2-6 months.<sup>[39,40]</sup> Thus, in all cases, it is advisable to get a CT and MRI. Radiological findings occur in three stages:<sup>[41]</sup>

- Stage I: Retropharyngeal abscess with ligamentous laxity, bony architecture of C1-C2 preserved
- Stage II: Ligamentous disruption with AAD, minimal bone destruction, and presence of retropharyngeal mass

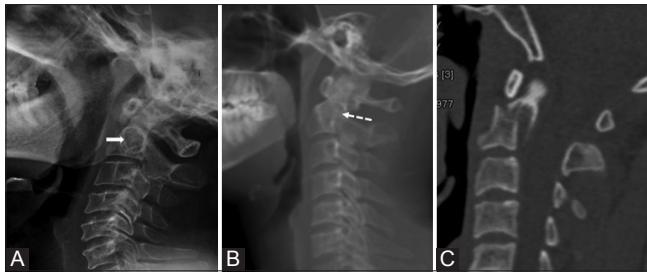


**Figure 13 (A-C):** The axis ring sign: Lateral cervical radiograph of a normal patient (A) Showing an intact axis ring (solid arrow). Plain radiograph (B) and corresponding sagittal CT (C) Image showing disruption of roof of the ring (dotted arrow) in a patient with road trauma suggestive of type III fracture. The ring remains intact in type II fracture

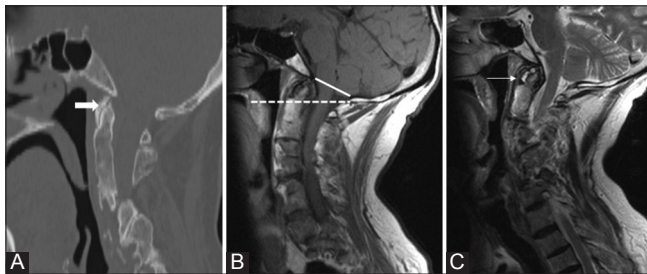


**Figure 15 (A-C):** Sagittal CT (A) Sagittal T1W and T2W MRI (B and C) Showing secondary degenerative changes in a patient with multiple segmentation anomalies. Reduced ADI (solid arrow) with sclerosis and osteophyte formation is seen. Fluid signal is noted in prevertebral space (arrow) which normally contains fat/soft tissue. Also seen is Group B Basilar invagination

- Stage III: Marked destruction of bone, complete obliteration of the anterior arch of C1 and complete loss of odontoid process, marked AAD, and occipito-atlantal instability.

Contrast Enhanced MRI especially better delineates the prevertebral, paravertebral, and epidural collections/granulation tissue [Figure 16]. Early changes of active bone involvement can be better picked up on MRI as altered signal on T1 and high signal intensity on T2 due to replacement of normal fat with inflammatory marrow edema.<sup>[42]</sup> In follow-up MRI, increase in the T1 intensity in the previously involved vertebra suggests recovery. Various treatment options available are antitubercular therapy (ATT) only, transoral decompression and posterior fusion, only posterior fusion, and traction.<sup>[38,39]</sup>

### Rheumatoid arthritis

Rheumatoid arthritis (RA) leads to inflammation of the synovial lining of the bursae and articular cartilage with formation of pannus, followed by destruction of cartilage and subchondral bone. It can cause marked thickening and fibrosis of dura and ligaments, and alternatively, decalcification and weakening of the ligament due to hyperemia<sup>[43]</sup> can cause ligament laxity and eventual lysis with corresponding mechanical instability. Around 20% of the patients with RA have AAD. However,



**Figure 14 (A-D):** Rotatory atlantoaxial subluxation: A child with h/o trauma followed by torticollis. VRT (A) and coronal and axial CT images showing dens lying eccentrically (B and C) in atlantal ring with anterior subluxation of lateral mass of C1 over C2 (D) Also note that AP axis of C1 and C2 are no more parallel

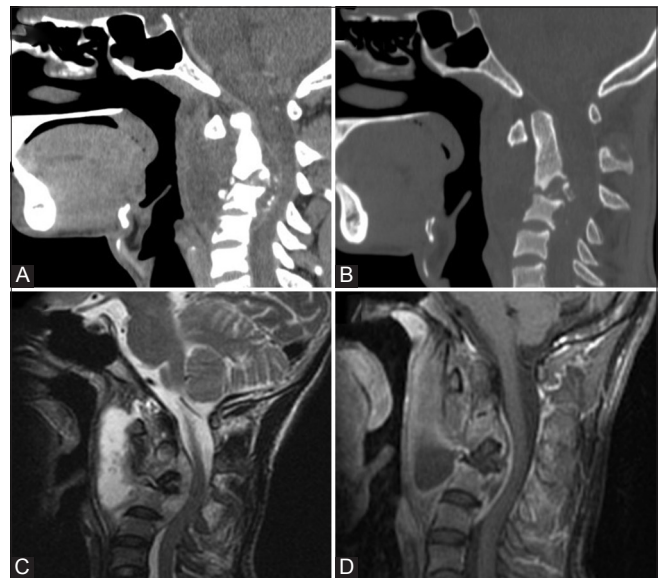


**Figure 16 (A-D):** Tuberculosis: Sagittal reformatted CT (A and B) Images show areas of osseous destruction involving the axis and C3 with associated prevertebral collection. Sagittal T2W (C) and sagittal post contrast T1W (D) MR images show rim enhancing prevertebral collection with epidural extension causing cord compression

only a small subset of patients develop neurological complications.<sup>[44]</sup>

The involvement of odontoid in RA may be seen as peridental pannus and prominent retrodental soft



tissue [Figure 17]. Thickening of ligaments (>3 mm) and erosions of dens are common. Rotatory as well as lateral AA subluxation, subaxial subluxation, brainstem compression, obliteration of subarachnoid space at AA level, and loss of fat that normally caps the dens are commonly seen.<sup>[44,45]</sup>

Cranial settling of odontoid<sup>[46]</sup> is said to be present when the superior aspect of the dens lies at or above the McRae line unless there is marked dental erosion, and the anterior arch of C1 assumes an abnormally low position in relation to C2.

Subaxial subluxation of C2 over C3 may be measured as either (i) the extent of subluxation measured in millimeters or (ii) the percentage of slip of one vertebra upon another. The sagittal diameter of the subaxial spinal canal better correlates with the presence and/or extent of myelopathy. Patients with subaxial canal diameters of 13 mm or less are at an increased risk of myelopathy.<sup>[47]</sup> Overall, the most common abnormalities seen are AAD and BI. Odontoid process osteoporosis, angulation, or fracture may also occur. Osteophyte formation is not seen due to deficient osteogenesis. Hook-like appearance of the odontoid due to erosions by pannus is characteristic of RA.

Dynamic contrast-enhanced MRI can also be done to characterize the type of pannus.<sup>[48]</sup> Spinal immobilization is the usual treatment of choice with systemic disease control. However, in patients with significant myelopathy, decompression may also be required.

### Ankylosing spondylitis

Ankylosing spondylitis (AS) is a chronic rheumatic disorder characterized by inflammation of the enthesis and sometimes the joints, which may lead to ankylosis. Neck involvement is classically thought to be common, especially in women and in patients with a long duration of disease.<sup>[49]</sup> Hip involvement is associated with more severe disease.<sup>[49,50]</sup>

Around 40-50% patients of AS have radiological changes in the cervical spine. Early spondylitis is characterized by small erosions at the corners of vertebral bodies with reactive sclerosis and vertebral body squaring. The most commonly

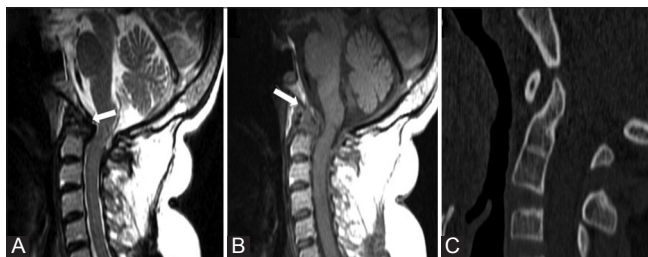


**Figure 17 (A-C): Rheumatoid Arthritis:** Sagittal T2 (A) and T1W MRI (B) Images showing T2 hypointense and T1 isointense pannus (arrows) and thickened TAL. There is destruction of odontoid and compression of cervicomedullary junction. Reformatted sagittal CT image (C) Showing Hook shaped odontoid in another patient with RA

observed lesion was the vertebral squaring, followed by facet joint involvement, syndesmophytes, vertebral body erosions, and discitis.<sup>[49]</sup> Diffuse syndesmophytic ankylosis can give a “bamboo spine” appearance and calcification of interspinous ligament gives a “dagger spine” appearance [Figure 18]. The fatty marrow within ossified disc is best seen on MRI. AA dislocation, fusion of zygoapophyseal joints, secondary atlanto-occipital assimilation, and spinal canal stenosis may also be seen as a part of disease process. Diffuse paraspinal ossification and inflammatory osteitis creates a fused, brittle spine, susceptible to fracture, even with minor trauma.

### CPPD

Calcium pyrophosphate dehydrogenase (CPPD) crystal deposition disease and crowned dens syndrome: CPPD crystal deposition disease is the third most common inflammatory arthritis, characterized by acute or chronic inflammation caused by deposit of CPPD crystals in articular cartilage and periarticular soft tissues, mostly in knees and wrists.<sup>[51,52]</sup> Like other soft tissues in the body, in upper cervical spine, TAL is also involved in crystal deposition.

Crowned dens syndrome (CDS) is a term frequently used in association with CPPD involvement of odontoid. CDS should be distinguished from calcification around the dens, which is only a radiographic entity without cervical pain.<sup>[53]</sup> CDS should be defined by characteristic clinical and radiographic findings. The typical clinical features of patients with CDS have been described as an acute onset of severe neck pain, restricted range of neck

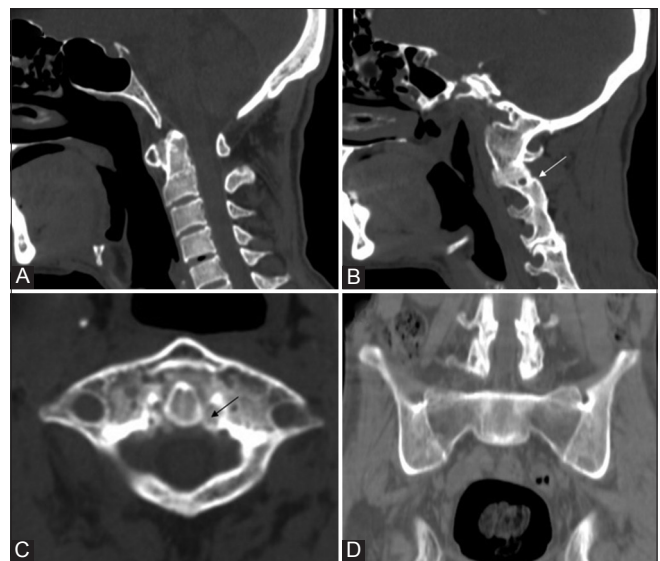


**Figure 18 (A-D): Ankylosing Spondylitis:** Reformatted Sagittal CT (A and B) Axial CT (C) and coronal pelvis CT (D) in a 34 year old HLA-B 27 positive male reveals atlanto-axial dislocation, ligament calcification (black arrow), fusion of zygoapophyseal joints (white arrow) and secondary atlanto-occipital assimilation with bilateral sacroiliac and hip joint ankylosis

motion (particularly of rotation), positive inflammatory indicators, and fever.

Calcification can develop anywhere around the odontoid process, including the synovial membrane, articular capsule, transverse ligament, cruciate and alar ligaments, although in around 90% cases, deposits occur posterior to the odontoid process. CT nicely demonstrates the calcific deposits around the dens in the transverse and alar ligaments, and in the anterior atlanto-occipital membrane. Horseshoe or crown-like calcification occurs surrounding the odontoid process. Other imaging features include subchondral cysts and erosions in odontoid.<sup>[54]</sup> Fracture line (usually type II) with signal changes suggestive of marrow edema may also be seen. Similar changes may be seen in axis body and atlas vertebra. This combination of subchondral cysts and erosions is specific as it is not seen in CPPD involvement of peripheral joints.<sup>[54,55]</sup> Retro-odontoid mass due to crystal deposition in TAL which appears hypointense to marrow signal on both T1 and T2WI, compressing the odontoid and causing erosion and destruction may be seen [Figure 19]. There may be secondary degenerative changes leading to narrowing, osteophytosis, sclerosis, and subluxation in the anteromedial part of AA joint. These may lead to cord changes due to contusion, myelomalacia, and ischemia.

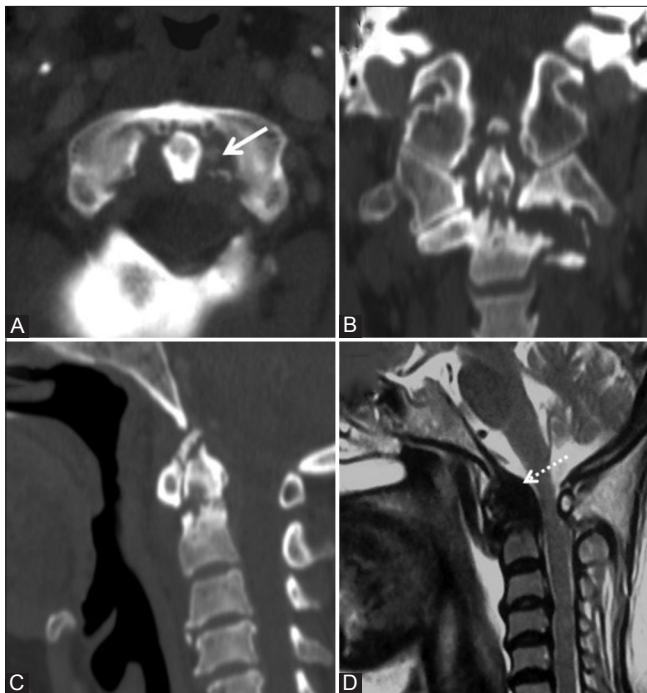


**Figure 19 (A-D): CPPD crystal deposition:** Reformatted CT images in all three planes (A-C) in a 64 year old female showing calcification of ligaments (solid arrow), type II pathological fracture of odontoid with erosions, sclerosis, osteophytes and narrowing of atlanto-dental interval. Hypointense retro-odontoid mass is seen on T2W MRI (D) images (dotted arrow) along with associated cord compression

The diagnosis is not always easy, as the symptoms are similar to those of other diseases, such as meningitis, cervicobrachial pain, occipitotemporal headache, calcific tendinitis of the longus colli muscle, spondylodiscitis, retropharyngeal abscess, polymyalgia rheumatica etc.<sup>[56]</sup> Patients show dramatic improvement with nonsteroidal anti-inflammatory drugs (NSAIDs) and colchicines.<sup>[55,56]</sup>

### Tumors

Neoplasms that involve dens may comprise osseous tumors arising within the dens and extension from soft tissue that surrounds the region. Metastatic malignancies, such as carcinoma of the breast, lung, prostate, kidney, thyroid, and multiple myeloma in adults; neuroblastoma, Ewing's tumor, leukemia, hepatoma, and retinoblastoma in children may also be seen [Figure 20].

### Miscellaneous Conditions and Associated Odontoid Anomalies

#### Down syndrome

CVJ anomalies in Down syndrome (DS) were first described in 1965 by Tishler and Martel, and are characterized by increased ligamentous laxity and abnormal joint anatomy.<sup>[57]</sup> Incidence of AA instability ranges between 7 and 20%; however, <1% of patients are symptomatic.<sup>[58]</sup> Patients may also have rotatory instability. Most common bone anomalies are os odontoideum (6%), followed by atlantal arch hypoplasia and bifid anterior or posterior arches. Dens is not secured against the anterior arch of C1 during flexion/extension. Occipitoatlantal instability is also frequently observed and may coexist with other anomalies.<sup>[58]</sup> Degenerative changes are common and occur early in patients with DS.

#### Morquio disease and other mucopolysaccharidosis

The various manifestations include odontoid process dysplasia-hypoplasia, AA instability or subluxation. Periodontoid tissue and ligament thickening due to deposition of mucopolysaccharide<sup>[59]</sup> is common that may

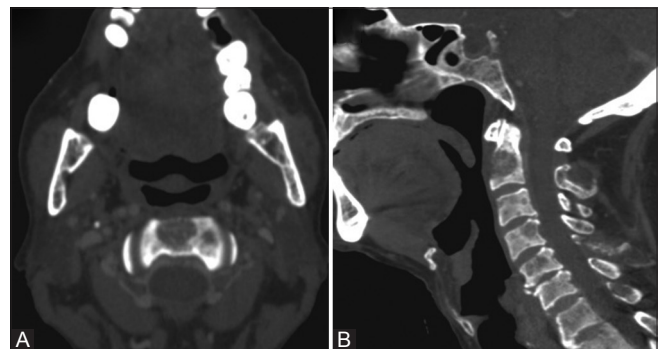


**Figure 20 (A and B): Multiple Myeloma:** Axial and reformatted sagittal CT images (A and B) Showing well defined punched out lytic lesion involving lower part of odontoid. Multiple other well defined lytic bony lesions were present in skull and spine

lead to spinal stenosis. These features represent a critical aspect in MPS (particularly in MPS IV) because if the spinal cord is compressed, cervical myelopathy may result and communicating hydrocephalus may be seen.<sup>[59-61]</sup> MRI is more appropriate for the evaluation of spinal cord alterations.

Other orthopedic manifestations include kyphoscoliosis and hip dysplasia.<sup>[62]</sup> Characteristic “J-shaped” conformation of the sella turcica is seen on the lateral view of the cranium.

### Klippel-Feil syndrome

Klippel-Feil syndrome is defined as congenital fusion of two or more cervical vertebrae and is believed to result from faulty segmentation along the embryo's developing axis during third to eighth weeks of gestation. Persons with Klippel-Feil syndrome may be at increased risk for spinal cord injury even after minor trauma due to hypermobility of the various cervical segments.<sup>[63]</sup>

Spectrum of anomalies include C1-C2 hypermobility and instability, BI, Chiari I malformation, diastematomyelia, and syringomyelia. Associated conditions are scoliosis, genito-urinary anomalies, Sprengel's deformity, cardiopulmonary involvement (mostly ventricular-septal defect), and deafness.<sup>[64]</sup> Management is usually conservative, rarely surgery is required.

Other less-common systemic associations of various odontoid anomalies are spondylo-epiphyseal dysplasia, achondroplasia, osteogenesis imperfecta, neurofibromatosis, rickets etc. and are beyond the scope of this review.

### Summary and Conclusion

Odontoid process is affected by a variety of congenital and acquired diseases. Imaging of this small structure to reach a specific diagnosis continues to be a challenge for radiologists. Multiplanar imaging with CT and MRI allows more detailed evaluation of bony and soft tissue structures. Adequate knowledge of development, complex anatomy, various disease processes, topographic relationships of odontoid with respect to CVJ and craniometry in association with appropriate clinical background can provide meaningful diagnosis.

### Acknowledgement

I acknowledge my parents, seniors, juniors, colleagues and my patients who helped and contributed every bit for compiling, writing, reviewing and for their critical feedback and support.

### Financial support and sponsorship

Nil.

### Conflicts of interest

There are no conflicts of interest.

### References

- Hensinger RN, Fielding JW, Hawkins RJ. Congenital anomalies of the odontoid process. *Orthop Clin North Am* 1978;9:901-12.
- Erbengi A, Oge HK. Congenital malformations of the craniovertebral junction: Classification and surgical treatment. *Acta Neurochir (Wien)* 1994;127:180-5.
- Redlund-Johnell I, Pettersson H. Radiographic measurements of the craniovertebral region. Designed for evaluation of abnormalities in rheumatoid arthritis. *Acta Radiol Diagn (Stockh)* 1984;25:23-8.
- McRae DL. Bony abnormalities in the region of the foramen magnum: Correlation of the anatomic and neurologic findings. *Acta Radiol* 1953;40:335-54.
- Chamberlain WE. Basilar impression (Platybasia): A bizarre developmental anomaly of the occipital bone and upper cervical spine with striking and misleading neurologic manifestations. *Yale J Biol Med* 1939;11:487-96.
- McGreger M. The significance of certain measurements of the skull in the diagnosis of basilar impression. *Br J Radiol* 1948;21:171-81.
- Smoker WR. MR imaging of the craniovertebral junction. *Magn Reson Imaging Clin N Am* 2000;8:635-50.
- Gupta V, Khandelwal N, Mathuria SN, Singh P, Pathak A, Suri S. Dynamic magnetic resonance imaging evaluation of craniovertebral junction abnormalities. *J Comput Assist Tomogr* 2007;31:354-9.
- Bhadelia RA, Bogdan AR, Wolpert SM. Analysis of cerebrospinal fluid flow waveforms with gated phase-contrast MR velocity measurements. *AJNR Am J Neuroradiol* 1995;16:389-400.
- Battal B, Kocaoglu M, Bulakbasi N, Husmen G, Tuba Sanal H, Tayfun C. Cerebrospinal fluid flow imaging by using phase-contrast MR technique. *Br J Radiol* 2011;84:758-65.
- Schweitzer ME, Hodler J, Cervilla V, Resnick D. Craniovertebral junction: Normal anatomy with MR correlation. *AJR Am J Roentgenol* 1992;158:1087-90.
- Wilms PL, Warwick R, Dyston M, Banister LH. *Gray's Anatomy*. 37<sup>th</sup> ed. Edinburgh: Churchill-Livingstone; 1989.
- Stevens JM, Chong WK, Barber C, Kendall BE, Crookard HA. A new appraisal of abnormalities of the odontoid process associated with atlanto-axial subluxation and neurological disability. *Brain* 1994;117:133-48.
- List CF. Neurological syndromes accompanying developmental anomalies of occipital bone, atlas and axis. *Arch Neurol Psychiatr* 1941;45:577-616.
- Wollin DG. The OS odontoideum. Separate odontoid process. *J Bone Joint Surg Am* 1963;45:1459-71.
- Rao PV, Mbajiorgu EF, Levy LF. Bony anomalies of the craniocervical junction. *Cent Afr J Med* 2002;48:17-23. Review.
- Pang D, Thompson DN. Embryology and bony malformations of the craniovertebral junction. *Childs Nerv Syst* 2011;27:523-64.
- Lustrin ES, Karakas SP, Ortiz AO, Cinnamon J, Castillo M, Vaheesan K, et al. Pediatric cervical spine: Normal anatomy, variants, and trauma. *Radiographics* 2003;23:539-60.
- Menezes AH. Embryology, development and classification of disorders of the Craniovertebral junction. In: Dickman CA, Sonntag VK, Spetzler RF, editors. *Surgery of the Craniovertebral Junction*. New York: Thieme Medical Publishers; 1998. p. 3-12.
- Nishikawa M, Sakamoto H, Hakuba A, Nakanishi N, Inoue Y. Pathogenesis of Chiari malformation: A morphometric study of the posterior cranial fossa. *J Neurosurg* 1997;86:40-7.
- Menezes AH. Craniocervical developmental anatomy and its implications. *Childs Nerv Syst* 2008;24:1109-22.
- Smoker WR. Craniovertebral junction: Normal anatomy, craniometry, and congenital anomalies. *Radiographics* 1994;14:255-77.
- Bajaj M, Jangid H, Vats A, Meena M. Case report: Congenital

- absence of the dens. *Indian J Radiol Imaging* 2010;20:109-11.
24. Phillips PC, Lorentsen KJ, Shropshire LC, Ahn HS. Congenital odontoid aplasia and posterior circulation stroke in childhood. *Ann Neurol* 1988;23:410-3.
  25. Arvin B, Fournier-Gosselin MP, Fehlings MG. Os odontoideum: Etiology and surgical management. *Neurosurgery* 2010;66(Suppl):22-31.
  26. Thomason M, Young JW. Case report 261:OS odontoideum (OO). *Skeletal Radiol* 1984;11:144-6.
  27. Von Torklus D, Gehle W. *The Upper Cervical Spine*. London: Butterworths; 1972.
  28. Vijayaradhi M, Phaniraj GL, Kumar BL. Anteverted odontoid: A rare congenital bony anomaly of craniovertebral junction. *Neurol India* 2010;58:490-2.
  29. Ryan MD, Henderson JJ. The epidemiology of fractures and fracture-dislocations of the cervical spine. *Injury* 1992;23:38-40.
  30. Smith L, Bauman JA, Grady M. *Neurosurgery*. In: Brunnicardi F, Andersen D, Billiar T, Dunn D, Hunter J, Matthews J, *et al.*, editors. *Schwartz's Principles of Surgery*. 9<sup>th</sup> ed. Chapter 42. New York, NY: McGraw-Hill Professional; 2010. p. 1583.
  31. Fielding JW, Cochran GV, Lawsing JF 3<sup>rd</sup>, Hohl M. Tears of the transverse ligament of the atlas. A clinical and biomechanical study. *J Bone Joint Surg Am* 1974;56:1683-91.
  32. Spence KF Jr, Decker S, Sell KW. Bursting atlantal fracture associated with rupture of the transverse ligament. *J Bone Joint Surg Am* 1970;52:543-9.
  33. Harris JH Jr, Burke JT, Ray RD, Nichols-Hostetter S, Lester RG. Low (type III) odontoid fracture: A new radiographic sign. *Radiology* 1984;153:353-6.
  34. Debernardi A, D'Aliberti G, Talamonti G, Villa F, Piparo M, Cenzato M. Traumatic (type II) odontoid fracture with transverse atlantal ligament injury: A controversial event. *World Neurosurg* 2013;79:779-83.
  35. Kowalski HM, Cohen WA, Cooper P, Wisoff JH. Pitfalls in the CT diagnosis of atlantoaxial rotary subluxation. *AJR Am J Roentgenol* 1987;149:595-600.
  36. Zapletal J, Hekster RE, Treurniet FE, de Valois JC, Wilmsink JT. MRI of atlanto-odontoid osteoarthritis. *Neuroradiology* 1997;39:354-6.
  37. Star MJ, Curd JG, Thorne RP. Atlantoaxial lateral mass osteoarthritis. A frequently overlooked cause of severe occipitocervical pain. *Spine (Phila Pa 1976)* 1992;17(Suppl):S71-6.
  38. Shukla D, Mongia S, Devi BI, Chandramouli BA, Das BS. Management of craniovertebral junction tuberculosis. *Surg Neurol* 2005;63:101-6.
  39. Sinha S, Singh AK, Gupta V, Singh D, Takayasu M, Yoshida J. Surgical management and outcome of tuberculous atlantoaxial dislocation: A 15-year experience. *Neurosurgery*. 2003 Feb; 52(2):331-8; discussion 338-9. PubMed PMID: 12535361.
  40. Behari S, Nayak SR, Bhargava V, Banerji D, Chhabra DK, Jain VK. Craniocervical tuberculosis: Protocol of surgical management. *Neurosurgery* 2003;52:72-81.
  41. Lifeso R. Atlanto-axial tuberculosis in adults. *J Bone Joint Surg Br* 1987;69:183-7.
  42. Krishnan A, Patkar D, Patankar T, Shah J, Prasad S, Bunting T, *et al.* Craniovertebral junction tuberculosis: A review of 29 cases. *J Comput Assist Tomogr* 2001;25:171-6.
  43. Roche CJ, Eyes BE, Whitehouse GH. The rheumatoid cervical spine: Signs of instability on plain cervical radiographs. *Clin Radiol* 2002;57:241-9.
  44. Narváez JA, Narváez J, Serrallonga M, De Lama E, de Albert M, Mast R, *et al.* Cervical spine involvement in rheumatoid arthritis: Correlation between neurological manifestations and magnetic resonance imaging findings. *Rheumatology (Oxford)* 2008;47:1814-9.
  45. Zikou AK, Argyropoulou MI, Alamanos Y, Tsifetaki N, Tsampoulas C, Voulgari PV, *et al.* Magnetic resonance imaging findings of the cervical spine in patients with rheumatoid arthritis. A cross-sectional study. *Clin Exp Rheumatol* 2005;23:665-70.
  46. Bundschuh C, Modic MT, Kearney F, Morris R, Deal C. Rheumatoid arthritis of the cervical spine: Surface-coil MR imaging. *AJR Am J Roentgenol* 1988;151:181-7.
  47. Boden SD. Rheumatoid arthritis of the cervical spine. Surgical decision making based on predictors of paralysis and recovery. *Spine (Phila Pa 1976)* 1994;19:2275-80.
  48. Stiskal MA, Neuhold A, Szolar DH, Saeed M, Czerny C, Leeb B, *et al.* Rheumatoid arthritis of the craniocervical region by MR imaging: Detection and characterization. *AJR Am J Roentgenol* 1995;165:585-92.
  49. El Maghraoui A, Bensabbah R, Bahiri R, Bezza A, Guedira N, Hajjaj-Hassouni N. Cervical spine involvement in ankylosing spondylitis. *Clin Rheumatol* 2003;22:94-8.
  50. Amor B, Santos RS, Nahal R, Listrat V, Dougados M. Predictive factors for the longterm outcome of spondyloarthropathies. *J Rheumatol* 1994;21:1883-7.
  51. Zhang W, Doherty M, Bardin T, Barskova V, Guerne PA, Jansen TL, *et al.* European League against rheumatism recommendations for calcium pyrophosphate deposition. Part I: Terminology and diagnosis. *Ann Rheum Dis* 2011;70:563-70.
  52. Ciapetti A, Filippucci E, Gutierrez M, Grassi W. Calcium pyrophosphate dihydrate crystal deposition disease: Sonographic findings. *Clin Rheumatol* 2009;28:271-6.
  53. Malca SA, Roche PH, Pellet W, Combalbert A. Crowned dens syndrome: A manifestation of hydroxy-apatite rheumatism. *Acta Neurochir (Wien)* 1995;135:126-30.
  54. Uri DS, Dalinka MK. Imaging of arthropathies. Crystal disease. *Radiol Clin North Am* 1996;34:359-74, xi.
  55. Salaffi F, Carotti M, Guglielmi G, Passarini G, Grassi W. The crowned dens syndrome as a cause of neck pain: Clinical and computed tomography study in patients with calcium pyrophosphate dihydrate deposition disease. *Clin Exp Rheumatol* 2008;26:1040-6.
  56. Aouba A, Vuillemin-Bodaghi V, Mutschler C, De Bandt M. Crowned dens syndrome misdiagnosed as polymyalgia rheumatica, giant cell arteritis, meningitis or spondylitis: An analysis of eight cases. *Rheumatology (Oxford)* 2004;43:1508-12.
  57. Tishler J, Martel W. Dislocation of the atlas in Mongolism: Preliminary report. *Radiology* 1965;84:904-6.
  58. Ali FE, Al-Bustan MA, Al-Busairi WA, Al-Mulla FA, Esbaita EY. Cervical spine abnormalities associated with Down syndrome. *Int Orthop* 2006;30:284-9.
  59. Kulkarni MV, Williams JC, Yeakley JW, Andrews JL, McArdle CB, Narayana PA, *et al.* Magnetic resonance imaging in the diagnosis of the cranio-cervical manifestations of the mucopolysaccharidoses. *Magn Reson Imaging* 1987;5:317-23.
  60. Thorne JA, Javadpour M, Hughes DG, Wraith E, Cowie RA. Craniovertebral abnormalities in Type VI mucopolysaccharidosis (Maroteaux-Lamy syndrome). *Neurosurgery* 2001;48:849-53.
  61. Zafeiriou DI, Batzios SP. Brain and spinal MR imaging findings in mucopolysaccharidoses: A review. *AJNR Am J Neuroradiol* 2013;34:5-13.
  62. White KK. Orthopaedic aspects of mucopolysaccharidoses. *Rheumatology (Oxford)* 2011;50(Suppl 5):v26-33.
  63. Ulmer JL, Elster AD, Ginsberg LE, Williams DW 3<sup>rd</sup>. Klippel-Feil syndrome: CT and MR of acquired and congenital abnormalities of cervical spine and cord. *J Comput Assist Tomogr* 1993;17:215-24.
  64. Hensinger RN, Lang JE, MacEwen GD. Klippel-Feil syndrome; a constellation of associated anomalies. *J Bone Joint Surg Am* 1974;56:1246-53.